



**Chapter 2:**

**Experimental and Theoretical Methods and  
Characterization Techniques**



This chapter deals with the materials, methodologies used for the synthesis of Schiff-base metal complexes in free as well as encapsulated states and their characterization techniques. The various techniques employed for the characterization of complexes include elemental analysis, atomic absorption spectroscopy (AAS), X-ray photoelectron spectroscopy (XPS), X-ray powder diffraction (XRD), scanning electron microscope (SEM), Fourier transform infrared (FTIR) spectroscopy, UV-visible spectroscopy and magnetic susceptibility measurement (SQUID) and catalytic studies are performed with the help of gas chromatography (GC). Furthermore, theoretical study is carried out to obtain better comprehension about the transition metal complexes both in ‘free’ and encapsulated states.

### 2.1 Material used

**Table 2.1:** List of the chemicals used in this study along with the name of their suppliers.

S.No.	Chemicals	Name of Supplier
1	Pure zeolite Y	Sigma-Aldrich, India
2	Nickel acetate	S.D. Fine, India
3	Palladium acetate	TCI chemicals, India
4	Copper acetate	S.D. Fine, India
5	Cobalt acetate	S.D. Fine, India
6	Ethylenediamine	Alfa-aesar
7	4-Hydroxy-salicylaldehyde	Alfa-aesar
8	5-Bromo- salicylaldehyde	Alfa-aesar
9	5-Hydroxy-salicylaldehyde	Alfa-aesar
10	5 -Methyl-salicylaldehyde	Alfa-aesar
11	5-Methoxy-salicylaldehyde	Alfa-aesar
12	Sodium chloride	Molychem
13	Silver acetate	Spectrochem
14	Aluminium isopropoxide	Spectrochem
15	Sodium meta silicate	CDH
16	Sulphuric acid	S.D. Fine, India
17	CTAB	Spectrochem
18	Ethanol	S.D. Fine, India
19	Methanol	S.D. Fine, India
20	Acetone	S.D. Fine, India
21	Diethyl ether	S.D. Fine, India
22	Styrene	Alfa-aesar
23	Thioanisol	Alfa-aesar
24	Rhodamine B	SDFCL
25	Hydrogen peroxide	Merck
26	Styrene oxide	Alfa-aesar
27	Phenyl bromide	Alfa-aesar
28	Barium Sulphate	Wako
29	Potassium bromide	SDFCL

### 2.2. Experimental Methods

#### 2.2.1. Synthesis of ligands (L1, L2, L3, L4, L5, L6):

To synthesize the ligand, two moles of salicylaldehyde or its derivatives are required to react with one mole of ethylene-diamine, so that the stoichiometric ratio is maintained in the product as shown in scheme 2.1.

#### Synthesis of *N,N'*-bis(salicylidene)ethylenediamine (L1)<sup>1</sup>

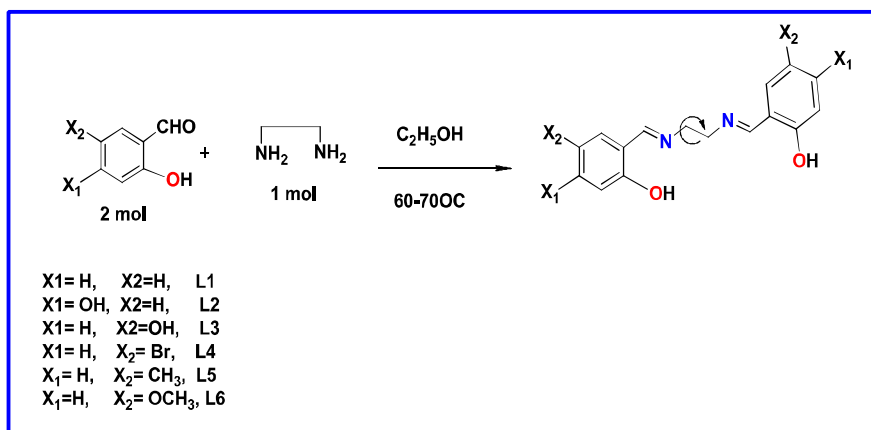
Two molar ratios of salicylaldehyde (5 mmol, 0.610 g) dissolved in ethanol is refluxed for (10-15) minutes. One molar ratio of ethylene-diamine (2.5 mmol, 0.33 ml) is added into it. The reaction mixture is refluxed for 30 minutes at (60 -70)°C and then ice cooled for an hour. Bright yellow solid flakes are obtained as product which is thoroughly washed with ethanol and then dried in air. The purity and structure of the compound is analyzed by its M.P. FT-IR and UV-visible spectroscopy.

#### 2.2.2 Synthesis of *N, N'*-bis(4-hydroxy-salicylidene)ethylenediamine (L2)<sup>1</sup>

To synthesize L2, 5 mmol, 0.690 g of 4-hydroxy-salicylaldehyde taken in ethanol is refluxed for (10-15) minutes. One molar ratio of ethylene-diamine (2.5 mmol, 0.33 ml) is added into it. The reaction mixture is further refluxed for 30 minutes at (60 -70)°C and then ice cooled for an hour. Bright yellow solid product is washed with ethanol and dried in air. The purity and structure of the compound is analyzed by M.P. FT-IR and UV-Vis spectroscopy.

#### 2.2.3 Synthesis of *N, N'*-bis(5-hydroxy-salicylidene)ethylenediamine (L3), *N, N'*-bis(5-bromo-salicylidene)ethylenediamine (L4), *N,N'*-bis(5-methyl-salicylidene)ethylenediamine (L5) and *N,N'*-bis(5-methoxy-salicylidene)ethylenediamine.<sup>1</sup>

For the synthesis of L3, L4, L5 and L6, 5-Hydroxy-salicylaldehyde (5 mmol, 0.690 g), 5-bromo-salicylaldehyde (5 mmol, 1.005g), 5-methyl-salicylaldehyde (5 mmol, 0.680g) and of 5-methoxy-salicylaldehyde (5 mmol, 0.760 g) are taken respectively. One molar ratio of ethylene-diamine (2.5 mmol, 0.33 ml) is added into the respective reaction and similar procedure (sections 2.2.1- 2.2.2) is followed for the synthesis of ligands.



**Scheme 2.1:** Schematic representation of synthesis of salen and derivative salen ligands.

### Analytical data of the synthesized ligands:

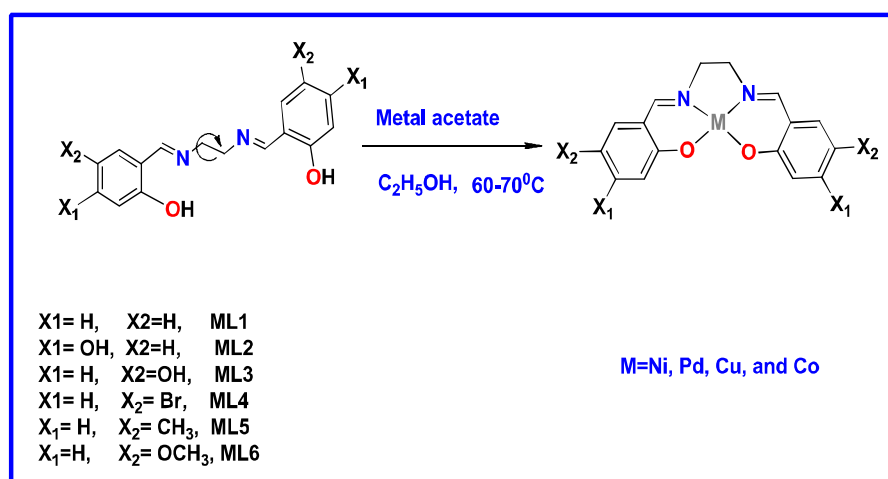
S. No.	Ligand	% Yield	M.P	IR data	UV-Vis data
1.	L1	94	126-128°C	(1633, C=N str.), (1557, 1488, C=C) str., (1374, C-H def), (1286, C-O str.).	( $\pi-\pi^*$ , 257) ( $n-\pi^*$ , 320)
2.	L2	82	180-183°C	(1641, C=N str.), (1583, 1471, C=C str.) (1363, C-H def.), (1229 C-O str.).	( $\pi-\pi^*$ , 255) ( $n-\pi^*$ , 324)
3.	L3	85	215-218°C	(1639, C=N str.), (1508, 1454, C=C str.), (1385, C-H def.), (1257, C-O str.)	( $\pi-\pi^*$ , 242 ) ( $n-\pi^*$ , 347)
4.	L4	96	184-186°C	(1633, C=N str.), (1572, 1481, C=C str.) (1390, C-H def.), (1361, C-O str.).	( $\pi-\pi^*$ , 252) ( $n-\pi^*$ , 331)
5.	L5	90	166-168°C	(1639, C=N str.), (1582, 1489, C=C str.), (1366, C-H def.), (1284, C-O str.)	( $\pi-\pi^*$ , 260) ( $n-\pi^*$ , 329)
6.	L6	80	164-165°C	(1639, C=N str.), (1589, 1494, C=C), (1325, C-H def.), (1272, C-O str.)	( $\pi-\pi^*$ , 247) ( $n-\pi^*$ , 346)

### 2.2.4. Synthesis of transition metals (Ni, Pd, Cu and Co) complexes.<sup>1</sup>

Ligands (L1, L2, L3, L4, L5 and L6 in the respective reactions) taken in ethanol is refluxed and then aqueous solution of equi molar ratio of desired metal salt is added in drop-wise fashion into it. The reaction mass is further refluxed for 30 minutes. For the synthesis of copper, palladium and cobalt Schiff-base complexes inert environment is used. The final product is recovered, washed with ethanol and diethyl ether and then dried at room temperature (Scheme 2.2).

### 2.2.5. Preparation of metal exchanged zeolites-Y.<sup>2,3</sup>

10 gram of pure Na-zeolite Y ( $\text{Na}_{58}\text{Al}_{58}\text{Si}_{136}\text{O}_{388}\cdot y\text{H}_2\text{O}$ ) is allowed to disperse in 0.01M metal salt ( $\text{Ni}(\text{CH}_3\text{COO})_2\cdot 2\text{H}_2\text{O} = 0.258\text{g}$ ,  $\text{Pd}(\text{CH}_3\text{COO})_2 = 0.224\text{g}$ ,  $\text{Cu}(\text{CH}_3\text{COO})_2=0.181\text{g}$  and  $\text{Co}(\text{CH}_3\text{COO})_2\cdot 4\text{H}_2\text{O} =0.177\text{g}$  ) in 100 ml water to acquire required loading level of desired metal ion, and stirred at room temperature for 24 hours. The slurry is filtered, washed repeatedly with water then desiccated for 12 hours at  $150^\circ\text{C}$  (Scheme 2.3).

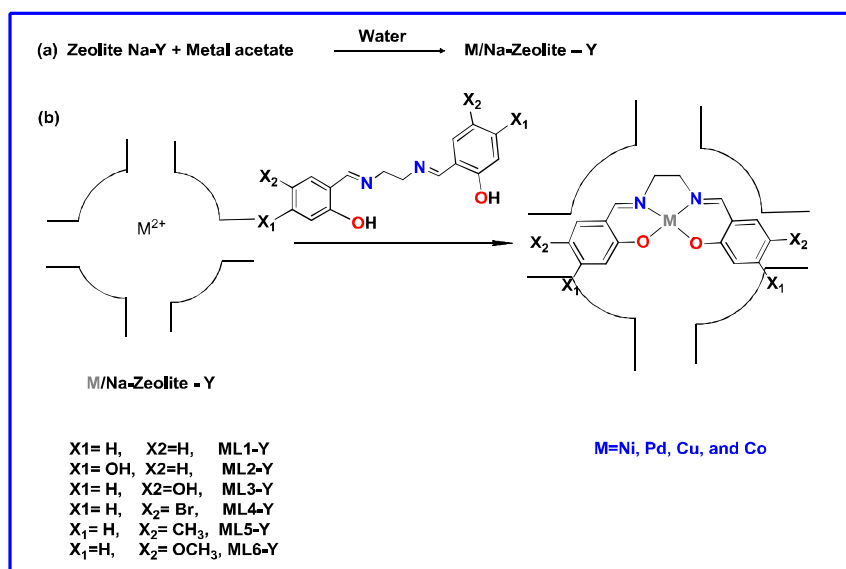


**Scheme 2.2:** Schematic representation of synthesis of ‘free state’ metal salen and its derivative complexes.

### 2.2.6. Synthesis of encapsulated of M(II) (Ni, Pd, Cu and Co) Schiff-base complexes in zeolite Y.<sup>4</sup>

Schiff-base ligands are flexible in nature, thus one of the methods of encapsulation of metal complexes inside the supercage of zeolite-Y could be possible via ‘flexible ligand’ approach (Scheme 2.3). The metal-exchanged zeolite and excess amount of ligand (L1, L2, L3, L4, L5 and L6 in each respective reaction) are allowed to react at  $200-250^\circ\text{C}$  for 24 hours, under

constant stirring to synthesize the complex inside the supercage of zeolite Y. The reaction mass is then recovered and further subjected to the Soxhlet extraction with the different solvents as acetone, methanol, and diethyl ether in a sequence. The product is dried in a muffle furnace for 10-12 hours at 150°C. Recovered material is further reacted with 0.01M NaCl solution for 12 hours to remove the unreacted metal ions, followed by filtration and washing until the filtrate has negative test for chloride ions.



**Scheme 2.3:** Schematic representation of synthesis of encapsulated metal salen and its derivative complexes.

(Detailed characterization of all the free state and zeolite encapsulated complexes are discussed in respective chapters, nickel complexes (chapter 3A, 3B and 3C), palladium complexes (chapter 4), copper complexes (chapter 5) and cobalt complexes (chapter 6).

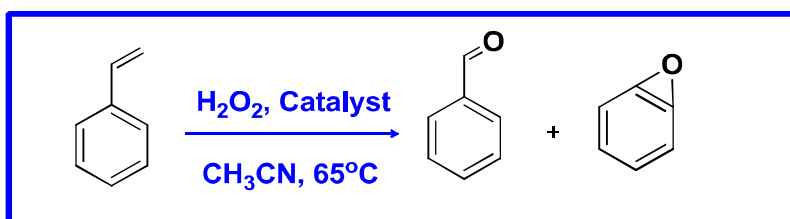
### 2.2.7. Synthesis of MCM-41

Synthesis of Al- MCM-41 is carried out according to the procedure<sup>5</sup> by keeping the molar ratio of sodium silicate and aluminum isopropoxide as 20: 1. For the synthesis of the Al-MCM-41 12.2 g (1 mol) sodium metasilicate (44–47% SiO<sub>2</sub>) dissolved in 50 g of deionized water and mixed with 1.1 g (0.05 mol) of aluminum isopropoxide (dissolved in 10 g of deionized water) solution. This mixture is stirred for 30 minutes after it and 100 ml of 1 N of sulfuric acid added maintaining the the same speed of stirring until gel formation takes place. After that, 7.2 g (0.2 mol) of cetyltrimethylammonium bromide is added drop by drop

through the addition funnel so that the gel changes into suspension. The suspension is transferred into polypropylene bottles and heated to 100°C for 4 days. After that, the material is cooled to room temperature, and recovered by filtration. The product is washed with deionized water and ethanol and finally calcined at 540°C for 12 hours.

### 2.2.8. Oxidation of Styrene.<sup>6</sup>

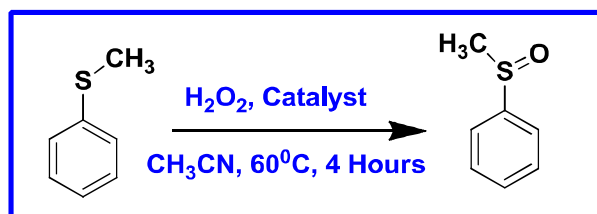
To carry out the catalytic oxidation of styrene, the substrate styrene (1.56 g, 15 mmol) and 30% H<sub>2</sub>O<sub>2</sub> (3.40 g, 30 mmol) are mixed with 15 ml acetonitrile and catalyst is taken in optimum amount at the temperature of 80°C for 8 hours (Scheme 2.4). The progress of reaction is monitored and quantified by gas chromatography by using internal standard (Phenyl bromide).



**Scheme 2.4:** Schematic representation of the formation of oxidation of styrene.

### 2.2.9. Sulfoxidation of methyl phenyl sulfide

Aqueous 30% H<sub>2</sub>O<sub>2</sub> (0.57 g, 5 mmol), methyl phenyl sulfide (0.62 g, 5 mmol) and catalyst (0.015 g) are mixed in minimum amount of solvent (3 ml of CH<sub>3</sub>CN) and the reaction mixture is stirred at 60°C temperature for four hours. The progress of the reaction is monitored by Gas Chromatography at different time intervals and the products are identified and quantified (by using internal standard method) with the help of GC (Scheme 2.5).



**Scheme 2.5:** Schematic representation of the formation of sulfoxidation from methyl phenyl sulphide.



### 2.2.10. Degradation of rhodamine B

Stock solution of Rhodamine B ( $1 \times 10^{-3}$  M) is prepared in 250 mL in deionized water. After dilution of this stock,  $1 \times 10^{-5}$  M solution of rhodamine B is prepared. 50 ml of rhodamine B ( $1 \times 10^{-5}$  M) solution is mixed with of  $\text{H}_2\text{O}_2$  (1mmol, 0.034g) and catalyst (0.05g), the mixture is irradiated under UV light (similar experiment is also carried out without use of  $\text{H}_2\text{O}_2$ ). After definite time intervals the absorbance of the solution is recorded instantaneously with the help of UV-Vis spectrometer. The absorbance value obtained in each case plotted against time to get the decomposition rate of dye and reactivity of catalysts.

### 2.3. Characterization Techniques

The instrumental techniques which are used for the detailed characterization of metal complexes in both states are summarized below.

#### 2.3.1 Powder X-ray diffraction (XRD)

Powder XRD is a scientific technique which uses X-ray on powder or micro crystalline samples for structural elucidation of that material. Cathode ray tube acts as the source of the X-ray, and before directed towards the sample, these rays are filtered to produce monochromatic radiation, collimated to concentrate.

The interaction in between the material and the incident X- rays produces constructive conclusions about crystal structure if they satisfy Bragg's equation.

$$\text{Bragg's equation} = 2d \sin \theta = n\lambda$$

Where  $n$  is a positive integer,  $\lambda$  is the wavelength of a beam of x-rays incident on a crystal with lattice planes separated by distance  $d$ , and  $\theta$  is the angle of incident rays. In present study, X-ray diffraction analysis has been performed with a RIGAKU MiniFlex II powder X-ray diffractometer ( from department of physics, BITS Piali) using  $\text{Cu K}\alpha$  radiation ( $\lambda = 1.542 \text{ \AA}$ ) within the  $2\theta$  range of  $8-50^\circ$  with the scanning rate of  $2^\circ/\text{min}$ . The XRD pattern of pure zeolite Y, metal-exchanged zeolite Y and zeolite Y encapsulated complexes have been studied. Comparative XRD studies of zeolite having encapsulated complex in it with the parent zeolite Y are significant to check out whether crystallinity of host zeolitic matrix is maintained even after the encapsulation of metal complex in zeolite Y.<sup>7,8</sup>



**Figure 2.1:** Photograph of powder X-ray diffractometer (RIGAKU MiniFlex II).

Where  $n$  is a positive integer,  $\lambda$  is the wavelength of a beam of x-rays incident on a crystal with lattice planes separated by distance  $d$ , and  $\theta$  is the angle of incident rays. In present study, X-ray diffraction analysis has been performed with a RIGAKU MiniFlex II powder X-ray diffractometer (from department of physics, BITS Pilani) using Cu  $K\alpha$  radiation ( $\lambda = 1.542 \text{ \AA}$ ) within the  $2\theta$  range of  $8\text{--}50^\circ$  with the scanning rate of  $2^\circ/\text{min}$ . The XRD pattern of pure zeolite Y, metal-exchanged zeolite Y and zeolite Y encapsulated complexes have been studied. Comparative XRD studies of zeolite having encapsulated complex in it with the parent zeolite Y are significant to check out whether crystallinity of host zeolitic matrix is maintained even after the encapsulation of metal complex in zeolite Y.<sup>7,8</sup>

### **2.3.2. Scanning Electron Microscopy and Energy Dispersive X-ray Spectroscopy (SEM-EDX)**

The scanning electron microscope (SEM) is an analytical technique which uses a high-energy electrons focused beam to generate a range of signals at the surface of solid sample. The signals originated because of the interactions of electron and sample reveal information about surface morphology, chemical composition and crystalline structure of materials. The SEM is also proficient technique to perform the analysis of selected point locations on the sample and it is very efficient approach to attain information qualitatively or semi-quantitatively for determination of chemical compositions (using EDX/EDS), crystalline structure, and crystal

orientations (using EBSD). In present thesis work, SEM-EDX has been performed by Zeiss EVO 40 (from IIT Roorkee, India) at an accelerated voltage of 5–20 kV, with gold coating. SEM images of parent zeolite Y and zeolites with the metal complexes entrapped inside have been recorded to investigate the surface morphology and elemental analysis of these investigated materials.



**Figure 2.2:** Photograph of Scanning Electron Microscope (Zeiss EVO 40).

### 2.3.3. X-ray Photo Electron Spectroscopy (XPS)<sup>9</sup>

X-ray photoelectron spectroscopy is a well known technique for the investigation of the surface chemistry of material. XPS technique can quantify the empirical formula, elemental composition, chemical and electronic states of the constituent's elements of the material of interest in attenuation depth of 20 Å. XPS spectra are acquired by irradiating a material surface with a beam of monoenergetic soft X-rays and energy analysing the electrons emitted by generally using Mg K $\alpha$  (1253.6eV) or Al K $\alpha$  (1486.6 eV) X-rays and at the same time by quantifying the electrons and kinetic energy which are emitted from the surface of material being analyzed.

In present study, X-ray photoelectron spectroscopic analysis has been performed using a commercial Omicron EA 125 spectrometer equipped with an Mg K $\alpha$  X-ray source (1253.6 eV) (from MNIT, Jaipur). Samples are prepared as pellets and are used after neutralization and the samples are out gassed in a vacuum oven overnight before XPS measurements. XP spectra of free and in zeolite encapsulated state have been recorded and all atoms in material

(except hydrogen) are recognized by identifying their corresponding binding energies in the particular chemical states.

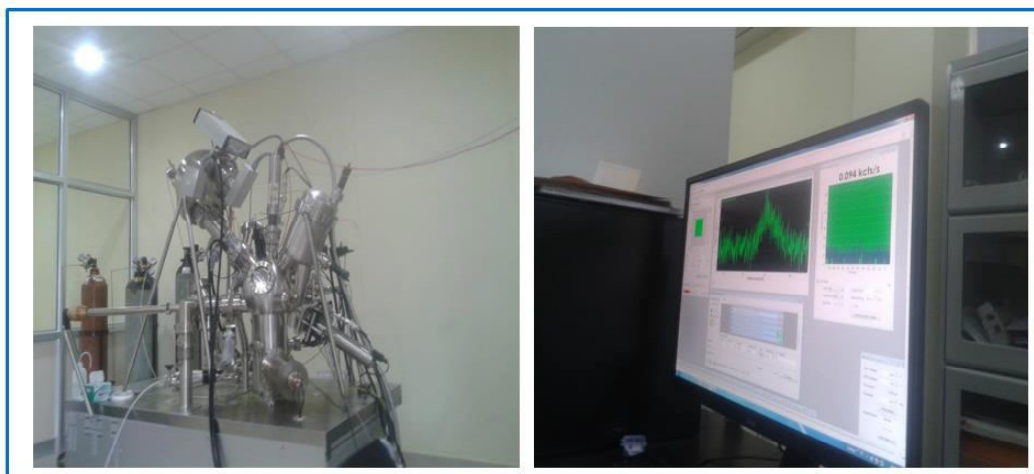


**Figure 2.3:** Photograph of X-ray photoelectron spectrophotometer (Omicron EA 125).

### 2.3.4. Infra-Red (IR) spectroscopy.<sup>10-12</sup>

Infrared spectroscopy deals with the interaction of infrared region of the electromagnetic spectrum with the matter. In this region associated photon energies (1 - 15 kcal/mole) are not adequate enough to excite the electrons; however, they may induce vibrational excitation in covalently bonded atoms and groups. According to gross selection rule of IR spectroscopy, an 'IR active' vibrational mode must be associated with changes in the electric dipole moment. The molecule need not to have permanent dipole moment however, requires only a change in dipole moment during the vibration. In the thesis work, infrared spectra ( $4000\text{-}450\text{ cm}^{-1}$ ) of Schiff base ligands, metal complexes, pure zeolite-Y, metal exchanged zeolite-Y and encapsulated complexes are recorded with KBr pallets on ABB FTIR spectrometer using a DRIFT accessory. This spectroscopic technique is primarily useful to characterize the functional groups and their chemical linkage in the ligands as well as their complexes in both states. Furthermore, this tool is also helpful specifically to study any change occurred in host lattice during the process of encapsulation.



**Figure 2.4:** Photograph of the Fourier Transform Infrared (FT-IR) spectrometer.

### 2.3.5. Electronic (UV-Visible) Spectroscopy

Electronic spectroscopy deals with the interactions of ultraviolet and visible radiations of electromagnetic spectrum with the matter and initiates electronic transitions by promotion of the electrons from their ground state to a high energy excited state. The wavelength of ultraviolet region falls in the range between 190-380 nm, the visible region fall between 380-750 nm. Many organic compounds as well as metal complexes can be characterized by the electronic spectroscopy. In present work, UV-visible spectra are recorded in solution and solid states of the complexes with the help of Shimadzu Spectrophotometer with model UV-2450. The solid state UV-Visible spectra are recorded using a Shimadzu UV- 2450 spectrophotometer with a diffuse reflectance attachment, which is outfitted with an integrating sphere of 60 mm inner diameter. The spectra are often recorded in the absorbance mode in the range of 190 nm to 700 nm using BaSO<sub>4</sub> as reference material. Some of solution state studies are also pursued with the help of JASCO model V-650 (Figure 2.4). Both spectrophotometers cover the wavelength range 190-900 nm, with two different lamps, tungsten (W-lamp) 900 to 350 nm and a deuterium (D<sub>2</sub>-lamp) has the range in 350-190 nm region. The light sources Si-photodiodes are used as the light detectors.



**Figure 2.5:** Photograph of the UV-Vis spectrophotometers (a) Shimadzu with model UV-2450 (b) JASCO with model V-650

### 2.3.6. Atomic absorption spectroscopy (AAS)



**Figure 2.6:** Photograph of Atomic Absorption Spectrophotometer (Shimadzu AA-7000).

Atomic absorption spectroscopy (AAS) is a spectroscopic technique for the quantitative determination of constituent elements of a material. This technique is based on the absorption

of optical radiation (light) by free atoms in the gaseous state and this is useful technique in analytical chemistry for determining the concentration of a particular element in a sample. In the present study we have used the Shimadzu AA-7000 spectrophotometer to determine the metal content of some of the nickel and palladium Schiff-base complexes in zeolite encapsulated state.

### 2.3.7. Superconducting quantum interference device (SQUID)

SQUID magnetometer is one of the most sensitive and effective ways of measuring magnetic properties. In particular, it is the only technique which is capable of determining the subtle magnetic moment of a sample. In this thesis, temperature dependent magnetic susceptibility studies of free and encapsulated state nickel and cobalt complexes have been carried out by using SQUID magnetometer Quantum Design MPMS XL Ever Cool (from IIT Roorkee, India), FC measurement in the field strength of 1000 Oe within temperature range of 5K to 300K.



**Figure 2.7:** Photograph of SQUID magnetometer Quantum Design MPMS XL Ever Cool.

### Calculation for the Molar Magnetic Susceptibility ( $X_m$ )

$$\text{Magnetic Susceptibility } (X) = \frac{\text{Magnetisation}(emu)}{\text{Magnetic field } (Oe)}$$

$$\text{Molar Magnetic Susceptibility}(X_m) = \frac{\text{Magnetic Susceptibility}(X)}{\text{Moles of metal centers}}$$

### Calculation of Magnetic Moment (BM)

$$= 2.82 * \sqrt{X_m} \times \sqrt{T}$$

### 2.3.8. Gas Chromatography (GC)

Gas chromatography (GC) is a well-established technique of analytical chemistry for the identification, separation and quantification of compounds that can be vaporized without decomposition. GC is a common type of chromatography and consists of the mobile phase as carrier gas (usually an inert gas such as helium, nitrogen) and the immobile phase (stationary phase) as a very thin layer of an inert liquid on an inert solid support such as beads of silica packed into a long thin tube and known as column. Compounds with a greater affinity for the mobile phase reach the detector at the end of the column and substance with a higher affinity for the stationary phase move gradually through the column. Thus, mixture to be analyzed is injected into the flow of carrier gas; it moves along the column and separated into the different substances according to their respective retention times.

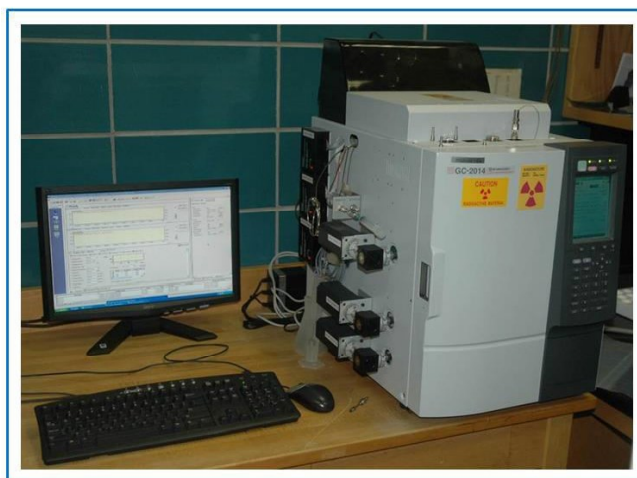


**Figure 2.8:** Photograph of GC-Shimadzu-2014.



### 2.3.9. Theoretical Methods

All Density Functional Theory (DFT) studies presented are done using GAUSSIAN 09 suite of *ab initio* quantum chemistry programs.<sup>13</sup> The structural optimizations used the hybrid B3PW91<sup>14, 15</sup> exchange and correlation functional with the double-zeta 6-31++G\*\* basis set for all atoms and consequently the same methodology is used for the vibrational frequency calculations to ascertain the stable isomers. All the complexes were also studied using B3LYP /6-31++G\*\* method as well and the results are found to be very similar.. Symmetry constraints are not imposed in structural optimizations, and default self-consistency and geometry convergence criteria were used for all studies. The electron density plots for frontier molecular orbitals, of the complexes in both singlet and triplet states are shown in the figures in respective sections. The molecular orbitals are defined with respect to the highest occupied molecular orbital (HOMO) and lowest unoccupied molecular orbital (LUMO) as HOMO-n (H-n) and LUMO+n (L+n). We have studied both the singlet and triplet spin states of the Ni-complexes, and the optical spectra for all the complexes are calculated using time dependent density functional theory (TD-DFT) employing B3PW91/6-31++G\*\* methods . SWizard software<sup>16, 17</sup> are used to analyze the transition energies and oscillator strengths for electronic excitations calculated (first 50 singlet or triplet excited states of the different complexes were calculated). In our theoretical studies, the geometrical relaxations of encapsulated Ni-complexes were done using 6-31G\*\* basis-set to ensure economical computer times along with acceptable results, and the TD-DFT spectra were calculated using 6-31++G\*\* basis-set keeping the complex geometry fixed. The geometrical optimizations of Ni complexes within the zeolite pore are started with an initial triplet structure, as switching of spin states during optimizations are not permissible. Triplet to triplet transitions are only considered for the triplet complexes, though pure d-d transitions are hard to identify due to strongly hybridized nature of the metal d-orbitals with ligand p orbitals for the encapsulated complexes. In the studies of encapsulation, we have modelled only a portion Zeolite-Y supercage as shown in corresponding figures and all the unsatisfied valancies of Si atoms are terminated using H atoms. The experimental structure of the zeolite supercage was taken without changes, and not relaxed, however the positions of the hydrogen atoms were optimized. In case of the studies with zeolite supercage with the complex encapsulated, only the complex inside the supercage was optimized and lowest energy structure was obtained.

### REFERENCES

1. S. Di Bella, I. Fragalà, I. Ledoux, M. A. Diaz-Garcia and T. J. Marks, *J. Am. Chem. Soc.*, 1997, **119**, 9550-9557.
2. N. Herron, *Inorg. Chem.*, 1986, **25**, 4714-4717.
3. K. Mori, M. Kawashima, K. Kagohara and H. Yamashita, *J. Phys. Chem. C*, 2008, **112**, 19449-19455.
4. K. K. Bania, D. Bharali, B. Viswanathan and R. C. Deka, *Inorg. Chem.*, 2012, **51**, 1657-1674.
5. M. Selvaraj, A. Pandurangan, K. S. Seshadri, P. K. Sinha, V. Krishnasamy and K. B. Lal, *J. Mol. Catal. A: Chem.*, 2002, **186**, 173-186.
6. M. R. Maurya, A. K. Chandrakar and S. Chand, *J. Mol. Catal. A: Chem.*, 2007, **274**, 192-201.
7. R. H. Jarman, *Zeolites*, 1985, **5**, 213-216.
8. K. K. Bania and R. C. Deka, *J. Phys. Chem. C*, 2013, **117**, 11663-11678.
9. J. Azoulay, *Vacuum*, 1983, **33**, 211-213.
10. G. Coudurier, C. Naccache and J. C. Vedrine, *J. Chem. Soc., Chem. Commun.*, 1982, DOI: 10.1039/C39820001413, 1413-1415.
11. E. M. Flanigen, H. Khatami and H. A. Szymanski, in *Molecular Sieve Zeolites-I*, AMERICAN CHEMICAL SOCIETY, 1974, vol. 101, ch. 16, pp. 201-229.
12. E. M. Flanigen and L. B. Sand, *Molecular Sieve Zeolites-I*, AMERICAN CHEMICAL SOCIETY, 1974.
13. M. Frisch, G. Trucks, H. Schlegel, G. Scuseria, M. Robb, J. Cheeseman, J. Montgomery Jr, T. Vreven, K. Kudin and J. Burant, *There is no corresponding record for this reference.*
14. A. D. Becke, *J. Chem. Phys.*, 1993, **98**, 5648-5652.
15. A. D. Becke, *Phys. Rev. A*, 1988, **38**, 3098-3100.
16. S. H. Lee, S. I. Gorelsky and G. I. Nikonov, *Organometallics*, 2013, **32**, 6599-6604.
17. J. P. Holland, P. J. Barnard, S. R. Bayly, J. R. Dilworth and J. C. Green, *Inorg. Chim. Acta*, 2009, **362**, 402-406.



**Chapter 3: Detailed Studies of Nickel Schiff-base  
Complexes Encapsulated in Zeolite Y**



This document was created with the Win2PDF "print to PDF" printer available at <http://www.win2pdf.com>

This version of Win2PDF 10 is for evaluation and non-commercial use only.

This page will not be added after purchasing Win2PDF.

<http://www.win2pdf.com/purchase/>